Published in final edited form as:
J Neurochem. 2010 March ; 112(5): 1286–1294. doi:10.1111/j.1471-4159.2009.06545.x.

Cholesterol modulates ion channels via down-regulation of phosphatidylinositol 4,5-bisphosphate

Yoon Sun Chun[*], **Sora Shin**[*], **Yonjung Kim**[*], **Hana Cho**[*], **Myoung Kyu Park**[*], **Tae-Wan Kim**[†], **Sergey V. Voronov**[†], **Gilbert Di Paolo**[†], **Byung-Chang Suh**[‡], and **Sungkwon Chung**[*]

[*]Department of Physiology, Samsung Biomedical Research Institute, Sungkyunkwan University School of Medicine, Suwon, South Korea

†Department of Pathology, Columbia University Medical Center, New York, NY, USA

‡Department of Physiology and Biophysics, University of Washington School of Medicine, Seattle, WA, USA

Abstract

Ubiquitously expressed Mg^{2+}-inhibitory cation (MIC) channels are permeable to Ca^{2+} and Mg^{2+} and are essential for cell viability. When membrane cholesterol level was increased by pre-incubating cells with a water-soluble form of cholesterol, the endogenous MIC current in HEK293 cells was negatively regulated. The application of phosphatidylinositol 4,5-bisphosphate (PIP_2) recovered MIC current from cholesterol effect. As PIP_2 is the direct modulator for MIC channels, high cholesterol content may cause down-regulation of PIP_2. To test this possibility, we examined the effect of cholesterol on two exogenously expressed PIP_2-sensitive K^+ channels: human *Ether-a-go-go* related gene (HERG) and KCNQ. Enrichment with cholesterol inhibited HERG currents, while inclusion of PIP_2 in the pipette solution blocked the cholesterol effect. KCNQ channel was also inhibited by cholesterol. The effects of cholesterol on these channels were blocked by pre-incubating cells with inhibitors for phospholipase C, which may indicate that cholesterol enrichment induces the depletion of PIP_2 via phospholipase C activation. Lipid analysis showed that cholesterol enrichment reduced γ-^{32}P incorporation into PIP_2 by approximately 35%. Our results suggest that cholesterol may modulate ion channels by changing the levels of PIP_2. Thus, an important cross-talk exists among two plasma membrane-enriched lipids, cholesterol and PIP_2.

Keywords

cholesterol; human *Ether-a-go-go* related gene; Mg^{2+}-inhibitory cation channel; phosphatidylinositol 4,5-bisphosphate; phospholipase C

Cholesterol constitutes a key component of the mammalian plasma membrane and is capable of influencing its structural and physical properties such as fluidity, curvature and stiffness. Therefore, cholesterol levels may affect the function of various ion channels and receptors in the plasma membrane. Cholesterol is known to be essential for the functionality of the nicotinic acetylcholine receptor because it is necessary for maintaining proper lipid–protein interaction (Fong and McNamee 1986). Manipulation of cholesterol content affects the equilibrium between the closed and open states of volume-regulated anion channels (Levitan *et al*. 2000). Similarly, cholesterol content affects the kinetic and steady-state parameters of activation and

Address correspondence and reprint requests to Professor Sungkwon Chung, PhD, Department of Physiology, Sungkyunkwan University School of Medicine, Suwon 440-746, South Korea. schung@med.skku.ac.kr.

inactivation of voltage-dependent K^+ (Kv1.3) channels in activated T lymphocytes (Hajdu *et al*. 2003), as well as structural coupling between L-type Ca^{2+} channels and adjacent regulatory proteins in ventricular myocytes (Tsujikawa *et al*. 2008). Cholesterol content has been shown to affect the gating of Ca^{2+}-activated K^+ channels in vascular smooth muscle cells (Chang *et al*. 1995). In some cases, cholesterol content regulates the formation of lipid raft micro-domain structures, thereby regulating the targeting of K^+ channels (Romanenko *et al*. 2004; Abi-Char *et al*. 2007), the activity of large-conductance Ca^{2+}-activated K^+ channels from colonic epithelia (Lam *et al*. 2004), and the surface expression of TRPC3 channels (Graziani *et al*. 2006). Collectively, these studies imply that cholesterol content may directly affect lipid–channel protein interactions, change channel gating kinetics and participate in targeting channels to specific micro-domains.

The various effects of cholesterol on ion channels are thought to occur through direct physical interactions with other lipids or target proteins. Alternatively, cholesterol may modulate ion channel activities by changing the signaling properties of the plasma membrane. For example, phosphoinositides (i.e. phosphorylated derivatives of phosphatidylinositol) are major signaling molecules found in the cell membrane. Among them, phosphatidylinositol 4,5-bisphosphate (PIP_2) plays a fundamental role in the plasma membrane, where it regulates signal transduction, exocytosis/endocytosis, actin dynamics, and ion channel and transporter function (Suh and Hille 2005; Di Paolo and De Camilli 2006). For instance, a large number of ion channels have been shown to be inhibited when PIP_2 is hydrolyzed by phospholipase C (PLC) (Suh and Hille 2005). In this study, we showed that increased cholesterol content decreases PIP_2 levels and inhibits PIP_2-sensitive channels, including the endogenous Mg^{2+}-inhibitory cation (MIC) channel and the exogenously expressed HERG K^+ and KCNQ K^+ channels. Cholesterol also acutely inhibited the HERG current. The inclusion of PIP_2 or PLC inhibitors in the pipette solution prevented acute inhibition by cholesterol. Also, pre-incubating cells with PLC inhibitors prevented cholesterol effect on these channels, indicating that increasing cholesterol levels activate the PLC pathway. Taken together, our results suggest that one of novel function of cholesterol is to modulate ion channels via regulation of PIP_2 level.

Materials and methods

All chemicals were purchased from Sigma-Aldrich (St Louis, MO, USA), except for U73122 (Research Biochemicals, Natick, MA, USA), *m*-3M3 fetal bovine serum (FBS), *o*-3M3FBS (Tocris, Ellisville, MO, USA) and edelfosine (Calbiochem, Gibbstown, NJ, USA). Phosphatidylinositol phosphates including DiC_8-PIP_2 and phosphatidic acid (PA) were dissolved in pipette solutions for whole-cell recordings and sonicated for 10 min at ice-cold temperature just before use.

Cell culture

Human embryonic kidney (HEK)293 cells were maintained in Dulbecco's modified Eagle's medium (DMEM) supplemented with 5% heat-inactivated FBS and penicillin/streptomycin at 37°C in a 5% CO_2 incubator. To enrich the cells with cholesterol, we exposed them to DMEM culture medium containing cholesterol water-solubilized with methyl-β-cyclodextrin (MβCD-cholesterol) for 1–2 h. During the incubation, cells were maintained in a humidified CO_2 incubator at 37°C. HERG cDNA was cloned into *Bam*HI/*Eco*RI sites of the plasmid pCDNA3.0 (Invitrogen, Carlsbad, CA, USA). DNA sequencing was used to verify the integrity of the HERG. HEK293 cells were transiently co-transfected with HERG-pCDNA3.0 and a green fluorescent protein cDNA plasmid (Clontech Laboratories, Mountain View, CA, USA) using the lipofectamine method (Invitrogen). Cells with green fluorescence were used for a patch clamp 24–48 h after transfection. For electrophysiologic analysis, cells were harvested with trypsinization, washed with phosphate-buffered saline (PBS), and studied within 8 h of harvest.

Human embryonic kidney tsA-201 (tsA) cells were cultured and transiently transfected using lipofectamine with various cDNAs: M1-muscarinic receptor and the channel subunits KCNQ2 and KCNQ3. TsA cells were maintained in DMEM supplemented with 10% FBS and 0.2% penicillin/streptomycin and used 24–48 h after transfection on poly-L-lysine-coated coverslips.

Cholesterol assay

Cells grown in 100 mm plates were assayed in duplicate for cholesterol using the Amplex red cholesterol assay kit (Molecular Probes, Eugene, OR, USA). First, cells were incubated for 2 h with MβCD-cholesterol, washed twice with ice-cold PBS and homogenized with hypotonic buffer (10 mM Tris-HCl, pH 7.5, 5 mM $MgCl_2$, 2 mM EGTA, 25 mM beta-glycerol phosphate, 5 mM sodium fluoride, 2 mM sodium pyrophosphate and 1 mM sodium orthovandate) using a 22-gauge needle. The samples were then centrifuged at 1000 *g* for 10 min to remove nuclei and cell debris. Membranes were pelleted from the post-nuclear supernatants by centrifugation for 1 h at 100 000 *g*, then assayed according to the supplier's instructions.

Cell viability assay

Cell viability was assessed by using a modified 3-(4,5-dimethylthiazol-2-yl)-2,5,diphenyl-tetrazolium bromide assay. Briefly, around 2×10^4 cells per well were seeded in 96-well microtiter plates with 100 μL of medium. After incubating cells in different conditions, 10 μL of 3-(4,5-dimethylthiazol-2-yl)-2,5,diphenyl-tetrazolium bromide (5 mg/mL stock in PBS) was added to each well and subsequently incubated for 1 h at 37°C. Absorption readings were performed at 540 nm with reference at 690 nm.

Electrophysiology

Patch pipettes were fabricated from borosilicate glass (TW150-4; World Precision Instrument, Sarasota, FL, USA) using a Flaming/Brown micropipette puller (P-97; Sutter Instrument, Novato, CA, USA). Patch-clamp experiments were conducted in a standard whole-cell recording configuration at 23–25°C. For MIC current, extracellular Na^+-based divalent cation-free recording solution contained: 130 mM sodium methanesulfonate, 5 mM NaCl, 10 mM HEPES and 12 mM N-hydroxyethyl-ethylenediamine-triacetic acid. pH was adjusted to 7.2 with NaOH. In the absence of divalent cations, MIC channels conduct large Na^+ inward current (Aarts *et al*. 2003). To prevent activation of Ca^{2+} release-activated Ca^{2+} (CRAC), the internal-free [Ca^{2+}] was buffered at 100 nM, calculated using Maxchelator software (Stanford University). The fully developed MIC current was almost completely blocked by 2-aminoethoxydiphenyl borate (Jeong *et al*. 2006), and the conductance decreased significantly by the presence of Ca^{2+} in extracellular solution as shown previously (Aarts *et al*. 2003). For the recording of CRAC current separately from MIC current, extracellular Ca^{2+}-containing bath solution was used, which contained: 135 mM sodium methanesulfonate, 3 mM $CaCl_2$, 0.5 mM EDTA and 10 mM HEPES. pH was adjusted to 7.2 with NaOH. Pipette solution contained: 135 mM Cs methanesulfonate, 10 mM 1,2-bis(2-aminophenoxy)ethane-N,N, N′,N ′-tetraacetic acid, 10 mM HEPES and 5 mM $MgCl_2$. Intracellular Mg^{2+} prevents the activation of MIC current (Hermosura *et al*. 2002). pH was adjusted to 7.2 with CsOH. Thapsigargin (1 μM) and inositol trisphosphate (IP_3;1 μM) were also included in pipette solution to deplete the intracellular Ca^{2+} store. For Kv current recordings, the bath solution contained: 140 mM NaCl, 3 mM $MgCl_2$, 10 mM HEPES, 5 mM KCl, 10 mM glucose (pH adjusted to 7.4 with NaOH). Pipette solution contained: 140 mM KCl, 5 mM NaCl, 1 mM $MgCl_2$, 10 mM HEPES, 5 mM EGTA, 2 mM Na-ATP and 1 mM Na-GTP (pH adjusted to 7.4 with KOH). Junction potentials were zeroed with the electrode in the standard bath solution.

Currents were amplified using an Axopatch 1D patch-clamp amplifier (Axon Instruments, Foster City, CA, USA). For KCNQ current and HERG current, transfected TsA cells and HEK cells were whole-cell clamped at 23–25°C, 24–48 h after transfection, as described previously

(Bian *et al*. 2001; Suh *et al*. 2006). Data were analyzed using pClamp7 (Axon Instruments) and the Origin 6.0 program (OriginLab, Northampton, MA, USA). For all experiments with individual cells, at least three independent batches of cells were used in different experimental days.

Thin layer chromatograph

Anion-exchange high-performance liquid chromatography analysis of phosphoinositides and phosphoinositide radiolabeling using liposomes and [γ^{32}P]ATP were performed as described (Berman *et al*. 2008). Radioactivity was quantified using a phosphorimager. In some experiments, cytosols were pre-incubated for 5 min at 37°C with 1 mM GDP or 0.2 mM GTP-γS. 'P2' subcellular fractions were prepared for metabolic labeling as follows: HEK cell was homogenized in 0.4 mL of 25 mM HEPES, pH 7.4, and 0.32 M sucrose (HEPES-based buffer), and centrifuged at 10 000 ×*g* in a microfuge. The resulting supernatant was diluted in 4 mL HEPES-based buffer and centrifuged at 45 000 ×*g* for 15 min at 4°C in an SS34 Sorvall centrifuge rotor. The pellet was re-suspended in 4 mL of 130 mM NaCl, 5 mM KCl, 2 mM $CaCl_2$, 2 mM $MgCl_2$, 25 mM HEPES (pH 7.33) and 30 mM glucose (control buffer) and re-centrifuged and re-suspended in the same buffer at a final protein concentration of 2 mg/mL. Aliquots of 100 μL were incubated with [^{32}P]orthophosphate at 2 mCi/mL for 30 min at 37° C. At the end of this incubation, samples were subjected to lipid extraction. Counts in the PIP_2 spot were normalized to those in the PA spot, which were not affected by the various genotypes. Lipids were extracted using chloroform/methanol (2 : 1) supplemented with 20 mg/mL cold phosphoinositides and processed for TLC.

ELISA for PIP_2

The amount of PIP_2 extracted from HEK293 cells were measured by using PIP_2 Mass ELISA kit (Echelon Biosciences Inc., Salt Lake City, UT, USA). PIP_2 was extracted from control or cholesterol-treated cell for 1 h at 150 μM. Cellular PIP_2 quantities were estimated by comparing the values from standard curve, which showed linear relationship at the range from 0.5 to 1000 pM concentrations.

Results

Inhibition of endogenous MIC currents by cholesterol via depletion of PIP_2

The transient receptor potential melastatin 7 (TRPM7)-associated MIC channel has been implicated in the control of cellular proliferation and viability by transporting various trace metal ions, in the regulation of Mg^{2+} and Ca^{2+}-homeostasis, and in anoxic neuronal death (Nadler *et al*. 2001; Aarts *et al*. 2003; Monteilh-Zoller *et al*. 2003; Schmitz *et al*. 2003). We measured endogenous MIC currents from HEK293 cells using the whole-cell patch clamp method in divalent cation-free bath solution. In agreement with a previous report (Jeong *et al*. 2006), MIC current recorded from control cells showed time-dependent activation, reaching a steady-state level approximately 400 s after obtaining whole-cell configuration (Fig. 1a). To determine if increasing the cholesterol level might regulate the activity of the MIC channel, we pre-incubated cells with 150 μM cholesterol water-solubilized with MβCD-cholesterol for 1–2 h prior to recordings. Under these conditions, membranous cholesterol levels increased by more than twofold, while no cell death was observed (data not shown). MIC currents were down-regulated by over 90% with this treatment, as shown in Fig. 1(a). However, the normalized current traces from control and cholesterol-enriched cells showed similar time-dependent activation, indicating that the activation rate of MIC currents was not changed by cholesterol enrichment (inset of Fig. 1a). Current-voltage relationships were obtained by applying ramp voltage pulses (Fig. 1b). Control cells showed slightly inward rectification, which is typical of MIC current. Cholesterol enrichment did not alter the shape of this curve, but reduced the currents at all voltages. These results suggest that cholesterol enrichment

decreases the number of activated MIC channels. When cells were pre-incubated with MβCD alone for 1–2 h to deplete cholesterol, MIC currents were increased by twofold, which was opposite to the effect of MβCD-cholesterol (data not shown). MβCD did not change the time-dependent activation rate of MIC currents. These results verified that the effects of MβCD and MβCD-cholesterol on MIC currents were specific for cholesterol.

It has been shown that PIP_2, but not its metabolites such as diacylglycerol and IP_3, directly modulates TRPM7 channels (Runnels *et al*. 2002). Specifically, the finding that PIP_2 depletion inhibits TRPM7 channels led us to hypothesize that down-regulation of endogenous MIC currents by cholesterol enrichment may be due to decreased levels of PIP_2. To test this possibility, we determined if increasing PIP_2 levels could restore normal MIC currents in cholesterol-enriched cells. When water soluble DiC_8-PIP_2 (25 μM) was directly applied to the cytoplasmic side of cells in the whole-cell configuration, MIC current was partially recovered as shown in Fig. 1(c). In contrast, application of the stereoisomer phosphatidylinositol 3,4-bisphosphate, PA, or phosphatidylinositol 3,4,5-trisphosphate was not as effective at rescuing MIC currents as PIP_2 at the same concentration (Fig. 1c). Next, the effect of cholesterol enrichment on other endogenous currents was tested in HEK293 cells. Neither CRAC current nor Kv current was inhibited by cholesterol enrichment (Fig. 1d). Thus, cholesterol enrichment inhibited MIC channels, but spared CRAC and Kv channels. Pre-incubating cells with MβCD alone for 1–2 h was without effect on CRAC current or Kv current (data not shown).

Inhibition of exogenously expressed HERG currents by cholesterol

To further test whether enhanced cholesterol levels down-regulate MIC currents by reducing PIP_2 levels, we investigated the effect of cholesterol-enrichment on other PIP_2-sensitive channels. K^+ currents were measured in HEK293 cells over-expressing the HERG K^+ channel, which has been implicated in the control of repolarization rate during the cardiac action potential (Bian *et al*. 2001). Exogenously expressed HERG K^+ channels gave rise to very slow activation behavior (Fig. 2a), as reported previously (Bian *et al*. 2001). Similar to the recordings for MIC currents, testing for the effect of cholesterol enrichment on the HERG K^+ current was carried out by pre-incubating cells with 150 μM water-soluble cholesterol for 1–2 h before recordings. Cholesterol enrichment inhibited the HERG K^+ current as shown in Fig. 2(a) for typical recordings. Increased cholesterol levels were inhibitory at all voltages tested, either when maximum currents were measured (Fig. 2b) or when tail currents were measured (Fig. 2c). The inclusion of 25 μM PIP_2 in the whole-cell pipette solution partially recovered HERG K^+ current from cholesterol-enriched cells (Fig. 2b and c). These results are consistent with a previous report showing that HERG K^+ current is under the regulation of PIP_2 (Bian *et al*. 2004), and they strongly suggest that increased cholesterol induces depletion of PIP_2.

A pharmacological approach was used to determine if the acute manipulation of endogenous PIP_2 levels could regulate HERG K^+ current. A major catabolic pathway for PIP_2 involves PLC-mediated hydrolysis of PIP_2 to generate diacylglycerol and IP_3 (Horowitz *et al*. 2005). We therefore used a PLC activator to down-regulate cellular PIP_2 levels. Figure 3(a) shows HERG K^+ current traces measured by step voltage pulses before and after the application of 25 μM *m*-3M3FBS, the active-form of PLC activator (Bae *et al*. 2003). The time-dependent change of current levels is shown in Fig. 3(b). Without drug treatment, control HERG K^+ currents showed little run-down during the recordings. In contrast, application of the PLC activator induced very rapid inhibition of the current, while the inactive-form, *o*-3M3FBS, was without effect. Based on these results, we confirmed that acute depletion of PIP_2 inhibits HERG K^+ current. We then tested the effect of acutely applied cholesterol on HERG K^+ currents. As shown in Fig. 3(c), current inhibition started approximately 5 min after the application of water-soluble cholesterol. About 20% of current inhibition was achieved within 15 min. Thus, even though cholesterol enrichment was less effective and required more time than the PLC activator

did, both treatments induced similar acute inhibition of HERG K^+ current. These results suggest that the inhibitory effect of cholesterol enrichment on HERG K^+ currents may occur via the activation of PLC. To test this hypothesis, we included PLC inhibitors in the whole-cell pipette solution. As shown in Fig. 3(c), the presence of PLC inhibitor, 10 μM edelfosine, in the pipette solution partially prevented the acute inhibitory effect of cholesterol. The acute effect of cholesterol was also prevented by the presence of structurally different PLC inhibitor, 5 μM U73122 (Fig. 3d). Inclusion of PIP_2 in the whole-cell pipette solution also prevented cholesterol effect (Fig. 3d), which may suggest that the acute depletion of PIP_2 suffices to suppress PIP_2-sensitive HERG channels. However, the effect of PIP_2 on the acute cholesterol inhibition was different from that of PIP_2 on cholesterol effect from whole-cell patches in Fig. 2(b).

It is possible that PIP_2-induced increase in HERG current from cholesterol-treated cell is completely independent of the inhibitory effect of cholesterol. Thus, the recovery of HERG current by PIP_2 could occur by the overlap between cholesterol-induced inhibition and PIP_2-induced facilitation. To test this possibility, we pre-incubated cells with PLC inhibitor edelfosine (5 μM) along with cholesterol for 1–2 h before recordings. As shown in Fig. 2(b) and (c), the addition of edelfosine prevented most of inhibitory effect of cholesterol on HERG current. Edelfosine alone was without effect on HERG current (data not shown). We also tested the effect of PLC inhibitors on the endogenous MIC currents. When 5 μM edelfosine or 1 μM U73122 were pre-incubated along with cholesterol, MIC current densities were 64.7 ± 6.0 pA/pF ($n = 9$) and 68.7 ± 7.5 pA/pF ($n = 8$), respectively. These values were similar to MIC current density from control cells (Fig. 1c). Therefore, the addition of PLC blockers prevented the inhibitory effect of cholesterol on MIC current as well. These results suggest that cholesterol enrichment inhibits either endogenous MIC current or exogenous HERG current via the membrane PIP_2 depletion by PLC activation.

Inhibition of KCNQ K^+ channels by cholesterol

Many cellular proteins, including ion channels and transporters, are inhibited when PIP_2 is hydrolyzed by PLC (Suh and Hille 2005). Although we showed that cholesterol enrichment depletes PIP_2, causing the down-regulation of PIP_2-sensitive MIC and HERG channels via the activation of PLC, we could not rule out other signaling molecules downstream of PLC or changes in other phospholipids. Recently, the depletion of PIP_2 has been shown to be sufficient to suppress KCNQ K^+ current without the need for other second messengers (Suh *et al.* 2006). Thus, we utilized HEK293-derived cell line tsA-201 cells expressing KCNQ channels to determine if cholesterol enrichment suppresses exogenously expressed KCNQ K^+ current. Families of current were elicited using voltage steps from –80 to +40 mV, in 10 mV intervals, in control and cholesterol-enriched cells (Fig. 4a). When voltage dependences of tail currents were compared, cholesterol-enriched cells showed a small rightward shift (data not shown). Deactivation and activation time constants were also increased by cholesterol enrichment. However, the most prominent effect of cholesterol enrichment on KCNQ K^+ channels was on current densities. When currents were measured immediately after whole-cell breakthrough, cholesterol-enriched cells showed only 27% of the current density level compared with control cells (Fig. 4b).

We tested the effects of PLC inhibitors on KCNQ K^+ currents. Pre-incubating cells with 2.5 μM U73122 or 2.5 μM edelfosine alone showed inhibitory effects on KCNQ K^+ currents as shown in Fig. 4(b). However, the presence of these blockers prevented the inhibitory effect of cholesterol on KCNQ K^+ currents (Fig. 4b). These results also suggest that cholesterol enrichment induces the depletion of PIP_2 via the activation of PLC. We also tested the acute effect of cholesterol on KCNQ K^+ currents. They showed slight rundown to 79% of the initial current at 20 min when measured at –20 mV (Fig. 4c). The acute application of cholesterol induced the inhibition of the current up to 53% of the initial current. In cells expressing M_1

muscarinic receptors, the application of muscarinic agonist oxotremorine-M following the application of cholesterol rapidly suppressed the current (Fig. 4d), confirming that depletion of PIP_2 inhibits KCNQ K^+ currents.

Down-regulation of PIP_2 by cholesterol

We analyzed phosphoinositide turnover using a cell-free radiolabeling assay in the presence of [γ-^{32}P] (Di Paolo *et al*. 2004), and tested the effect of cholesterol enrichment on PIP_2 levels. We analyzed extracts prepared from control and cholesterol-enriched HEK293 cells using TLC (Fig. 5a) and found a 35% reduction in γ-^{32}P incorporation into PIP_2 in cholesterol-enriched cells, relative to control cells ($n = 4$; Fig. 5b). A considerable decrease in PA labeling was also observed in cholesterol-enriched cells, while there was no change in the labeling of phosphatidylinositol phosphates. Incorporation of radioactive phosphate into phospholipids could occur through lipid kinase-mediated phosphorylation, as well as through contributions from phosphatases and phospholipases. PIP_2 levels at steady state were also measured by using PIP_2 ELISA kit from HEK293 cells. Compared with control cells, cholesterol-enriched HEK293 cells showed 18.1 ± 0.4% ($n = 6$) reduction in PIP_2 level. Thus, our lipid analysis indicates that cholesterol enrichment depletes PIP_2 by either diminishing synthesis or enhancing breakdown of PIP_2.

Discussion

In this study, we show that cholesterol enrichment inhibits PIP_2-sensitive channels by down-regulating PIP_2 levels. We tested the effects of cholesterol on one of the endogenous non-selective channels (MIC) and two different exogenously expressed K^+ channels (HERG and KCNQ). All of these channels are known to be positively regulated by PIP_2.Asa growing number of channels are known to be under the regulation of PIP_2 (Suh *et al*. 2006), the activities of all these channels may be affected by plasma membrane cholesterol. However, the extent of modulation may not only be dependent on the expression of these ion channels in specific cells, but also on the sensitivity of a specific channel to PIP_2, because the regulation of ion channels by PIP_2 is dependent on the apparent affinity of the channel protein for PIP_2 (Gamper and Shapiro 2007).

Increasing PIP_2 levels restored MIC (Fig. 1c) and HERG currents (Fig. 2b and c) in cholesterol-enriched cells. In addition, addition of PLC inhibitors or PIP_2 to the pipette solution prevented the acute inhibitory effect of cholesterol on HERG K^+ current (Fig. 3d). Also, we confirmed that the presence of PLC inhibitors prevented most of cholesterol effect on all of three channels tested. Thus, these results suggest that depletion of PIP_2 by cholesterol enrichment may occur through the activation of PLC. Activation of PLC by cholesterol was previously suggested to explain the mitogen-like action of cholesterol on ascites tumor cell growth and macromolecule synthesis (Haeffner and Wittmann 1999). Cholesterol enrichment may induce activation of PLC through several mechanisms. First, cholesterol may induce translocation of some PLC isoforms from the cytosol to the plasma membrane, where breakdown of PIP_2 may occur. Intracellular translocation of phosphoinositide-specific PLC-δ isoform to the cell surface is known to be cell cycle-dependent (Yagisawa *et al*. 2006). Second, cholesterol may activate PLC by promoting its phosphorylation (Kim *et al*. 2000). Third, cholesterol may increase the expression levels of PLC. We are currently investigating these possibilities.

Although PIP_2 is a minor component in the plasma membrane, it plays important regulatory roles in a variety of cell functions, such as rearrangement of the cytoskeleton and membrane trafficking (Di Paolo and De Camilli 2006). To explain the multiple roles of PIP_2, the concept of spatially confined PIP_2 pools was proposed (Janmey and Lindberg 2004). Cholesterol- and sphingolipid-rich rafts may serve to confine PIP_2 within the plasma membrane. Thus, the confinement of PIP_2 to rafts may allow PIP_2 hydrolysis to occur locally and restrict signaling

mechanisms to the site of activation (Pike and Miller 1998; Hur *et al*. 2004). However, this hypothesis, termed 'raft-delimited PIP_2 signaling,' has been disputed recently (van Rheenen *et al*. 2005). It is possible that the steady-state level of PIP_2 is determined by the concerted action of phosphoinositide kinases and phosphatases. Our results may suggest another way of regulating PIP_2 levels within specific micro-domains. Cholesterol content in a specific micro-domain may regulate PIP_2 levels via PLC activity. Interestingly, PLCb1 is shown to localize in detergent-resistant membrane microdomain prepared from synaptic plasma membrane fraction of rat brain (Taguchi *et al*. 2007).

It has been suggested that cholesterol plays a crucial role in the development and maintenance of neuronal plasticity and function (Pfrieger 2003). Failure of cholesterol homeostasis has been suggested as the unifying cause of synaptic degeneration (Koudinov and Koudinova 2005). For example, there is evidence suggesting that cholesterol levels are closely connected to neurological disorders such as Alzheimer's disease (Puglielli *et al*. 2003). When cholesterol homeostasis is compromised in such neurodegenerative conditions, perturbation of PIP_2 levels may follow, according to our results. Consequently, the activities of PIP_2-sensitive ion channels change, leading to modifications not only in passive ionic permeability, but also in the active properties of the neurons, such as their action potentials. Interestingly, we found that the activation of MIC channels is chronically suppressed by the presence of familial Alzheimer's disease-associated mutant presenilin (Landman *et al*. 2006). The down-regulation of PIP_2 contributes to the observed channel deficits, as well as to the generation of amyloidogenic β-amyloid peptide, Aβ42. Alternatively, a recent report has shown that the oligomeric form of Aβ decreases the level of PIP_2, resulting in synaptic dysfunction (Berman *et al*. 2008). These results suggest that PIP_2 may serve as the molecule linking cholesterol metabolism to the pathogenesis of Alzheimer's disease. Thus, membrane cholesterol content may share the same molecular mechanism with Alzheimer's disease-causing presenilin mutations (i.e. down-regulation of PIP_2).

Acknowledgments

This work was also supported by Samsung Biomedical Research Grant and Korea Research Foundation Grant funded by NIH grant R01 NS056049 (G.D.P.) and the Korean Government (KRF-2006-E00009) to S.C.

Abbreviations used

CRAC	calcium release-activated calcium
DMEM	Dulbecco's modified Eagle's medium
DMSO	dimethylsulfoxide
FBS	fetal bovine serum
HEK	human embryonic kidney
HERG	human *Ether-a-go-go* related gene
IP_3	inositol trisphosphate
Kv current	voltage-dependent K^+ current
MIC	Mg^{2+}-inhibitory cation channel
MβCD	methyl-β-cyclodextrin
PA	phosphatidic acid
PBS	phosphate-buffered saline
PIP_2	phosphatidylinositol 4,5-bisphosphate

PLC	phospholipase C
TRPM7	transient receptor potential melastatin 7

References

Aarts M, Iihara K, Wei WL, Xiong ZG, Arundine M, Cerwinski W, MacDonald JF, Tymianski M. A key role for TRPM7 channels in anoxic neuronal death. Cell 2003;115:863–877. [PubMed: 14697204]

Abi-Char J, Maguy A, Coulombe A, Balse E, Ratajczak P, Samuel JL, Nattel S, Hatem SN. Membrane cholesterol modulates Kv1.5 potassium channel distribution and function in rat cardiomyocytes. J. Physiol 2007;582:1205–1217. [PubMed: 17525113]

Bae YS, Lee TG, Park JC, Hur JH, Kim Y, Heo K, Kwak JY, Suh PG, Ryu SH. Identification of a compound that directly stimulates phospholipase C activity. Mol. Pharmacol 2003;63:1043–1050. [PubMed: 12695532]

Berman DE, Dall'Armi C, Voronov SV, et al. Oligomeric amyloid-beta peptide disrupts phosphatidylinositol-4,5-bisphosphate metabolism. Nat. Neurosci 2008;11:547–554. [PubMed: 18391946]

Bian J, Cui J, McDonald TV. HERG K^+ channel activity is regulated by changes in phosphatidyl inositol 4,5-bisphosphate. Circ. Res 2001;89:1168–1176. [PubMed: 11739282]

Bian JS, Kagan A, McDonald TV. Molecular analysis of PIP_2 regulation of HERG and IKr. Am. J. Physiol. Heart Circ. Physiol 2004;287:H2154–H2163. [PubMed: 15231497]

Chang HM, Reitstetter R, Mason RP, Gruener R. Attenuation of channel kinetics and conductance by cholesterol: an interpretation using structural stress as a unifying concept. J. Membr. Biol 1995;143:51–63. [PubMed: 7714888]

Di Paolo G, De Camilli P. Phosphoinositides in cell regulation and membrane dynamics. Nature 2006;443:651–657. [PubMed: 17035995]

Di Paolo G, Moskowitz HS, Gipson K, et al. Impaired PtdIns(4,5)P2 synthesis in nerve terminals produces defects in synaptic vesicle trafficking. Nature 2004;431:415–422. [PubMed: 15386003]

Fong TM, McNamee MG. Correlation between acetylcholine receptor function and structural properties of membranes. Biochemistry 1986;25:830–840. [PubMed: 3008814]

Gamper N, Shapiro MS. Regulation of ion transport proteins by membrane phosphoinositides. Nat. Rev. Neurosci 2007;8:921–934. [PubMed: 17971783]

Graziani A, Rosker C, Kohlwein SD, Zhu MX, Romanin C, Sattler W, Groschner K, Poteser M. Cellular cholesterol controls TRPC3 function: evidence from a novel dominant-negative knockdown strategy. Biochemical J 2006;396:147–155.

Haeffner EW, Wittmann U. Cholesterol-induced growth stimulation, macromolecule synthesis, and increased phosphoinositide metabolism of ascites tumour cells in culture. Cell. Signal 1999;11:821–829. [PubMed: 10617285]

Hajdu P, Varga Z, Pieri C, Panyi G, Gaspar R Jr. Cholesterol modifies the gating of Kv1.3 in human T lymphocytes. Pflugers Arch 2003;445:674–682. [PubMed: 12632187]

Hermosura MC, Monteilh-Zoller MK, Scharenberg AM, Penner R, Fleig A. Dissociation of the store-operated calcium current I_{CRAC} and the Mg-nucleotide-regulated metal ion current MagNum. J. Physiol 2002;539:2.

Horowitz LF, Hirdes W, Suh BC, Hilgemann DW, Mackie K, Hille B. Phospholipase C in living cells: activation, inhibition, Ca^{2+} requirement, and regulation of M current. J. Gen. Physiol 2005;126:243–262. [PubMed: 16129772]

Hur EM, Park YS, Lee BD, Jang IH, Kim HS, Kim TD, Suh PG, Ryu SH, Kim KT. Sensitization of epidermal growth factor-induced signaling by bradykinin is mediated by c-Src. Implications for a role of lipid microdomains. J. Biol. Chem 2004;279:5852–5860. [PubMed: 14630916]

Janmey PA, Lindberg U. Cytoskeletal regulation: rich in lipids. Nat. Rev. Mol. Cell Biol 2004;5:658–666. [PubMed: 15366709]

Jeong SY, Shin SY, Kim HS, Bae CD, Uhm DY, Park MK, Chung S. Regulation of magnesium-inhibited cation current by actin cytoskeleton rearrangement. Biochem. Biophys. Res. Commun 2006;339(3): 810–815. [PubMed: 16325775]

Kim MJ, Kim E, Ryu SH, Suh PG. The mechanism of phospholipase C-gamma1 regulation. Exp. Mol. Med 2000;32:101–109. [PubMed: 11048639]

Koudinov AR, Koudinova NV. Cholesterol homeostasis failure as a unifying cause of synaptic degeneration. J. Neurol. Sci 2005;229:233–240. [PubMed: 15760645]

Lam RS, Shaw AR, Duszyk M. Membrane cholesterol content modulates activation of BK channels in colonic epithelia. Biochim. Biophys. Acta 2004;1667:241–248. [PubMed: 15581861]

Landman N, Serban G, Shin SY, Kang MS, Chung S, Kim T-W. Presenilin mutations linked to familial Alzheimer's disease cause an imbalance in phosphatidylinositol 4,5-bisphosphate metabolism. Proc. Natl. Acad. Sci. USA 2006;103:19524–19529. [PubMed: 17158800]

Levitan I, Christian AE, Tulenko TN, Rothblat GH. Membrane cholesterol content modulates activation of volume-regulated anion current in bovine endothelial cells. J. Gen. Physiol 2000;115:405–416. [PubMed: 10736308]

Monteilh-Zoller MK, Hermosura MC, Nadler MJ, Scharenberg AM, Penner R, Fleig A. TRPM7 provides an ion channel mechanism for cellular entry of trace metal ions. J. Gen. Physiol 2003;121:49–60. [PubMed: 12508053]

Nadler MJ, Hermosura MC, Inabe K, et al. LTRPC7 is a Mg.ATP-regulated divalent cation channel required for cell viability. Nature 2001;411:590–595. [PubMed: 11385574]

Pfrieger FW. Cholesterol homeostasis and function in neurons of the central nervous system. Cell. Mol. Life Sci 2003;60:1158–1171. [PubMed: 12861382]

Pike LJ, Miller JM. Cholesterol depletion delocalizes phosphatidylinositol bisphosphate and inhibits hormone-stimulated phosphatidylinositol turnover. J. Biol. Chem 1998;273:22298–22304. [PubMed: 9712847]

Puglielli L, Tanzi RE, Kovacs DM. Alzheimer's disease: the cholesterol connection. Nat. Neurosci 2003;6:345–351. [PubMed: 12658281]

van Rheenen J, Achame EM, Janssen H, Calafat J, Jalink K. PIP_2 signaling in lipid domains: a critical re-evaluation. EMBO J 2005;24:1664–1673. [PubMed: 15861130]

Romanenko VG, Fang Y, Byfield F, Travis AJ, Vandenberg CA, Rothblat GH, Levitan I. Cholesterol sensitivity and lipid raft targeting of Kir2.1 channels. Biophys. J 2004;87:3850–3861. [PubMed: 15465867]

Runnels LW, Yue L, Clapham DE. The TRPM7 channel is inactivated by PIP_2 hydrolysis. Nat. Cell Biol 2002;4:329–336. [PubMed: 11941371]

Schmitz C, Perraud AL, Johnson CO, Inabe K, Smith MK, Penner R, Kurosaki T, Fleig A, Scharenberg AM. Regulation of vertebrate cellular Mg^{2+} homeostasis by TRPM7. Cell 2003;114:191–200. [PubMed: 12887921]

Suh BC, Hille B. Regulation of ion channels by phosphatidylinositol 4,5-bisphosphate. Curr. Opin. Neurobiol 2005;15:370–378. [PubMed: 15922587]

Suh BC, Inoue T, Meyer T, Hille B. Rapid chemically induced changes of PtdIns(4,5)P2 gate KCNQ ion channels. Science 2006;314:1454–1457. [PubMed: 16990515]

Taguchi K, Kumanogoh H, Nakamura S, Maekawa S. Localization of phospholipase Cβ1 on the detergent-resistant membrane microdomain prepared from synaptic plasma membrane fraction of rat brain. J. Neurosci. Res 2007;85:1364–1371. [PubMed: 17348042]

Tsujikawa H, Song Y, Watanabe M, Masumiya H, Gupte SA, Ochi R, Okada T. Cholesterol depletion modulates basal L-type Ca^{2+} current and abolishes its β-adrenergic enhancement in ventricular myocytes. Am. J. Physiol. Heart Circ. Physiol 2008;294:H285–H292. [PubMed: 17982015]

Yagisawa H, Okada M, Naito Y, Sasaki K, Yamaga M, Fujii M. Coordinated intracellular translocation of phosphoinositidespecific phospholipase C-delta with the cell cycle. Biochim. Biophys. Acta 2006;1761:522–534. [PubMed: 16580873]

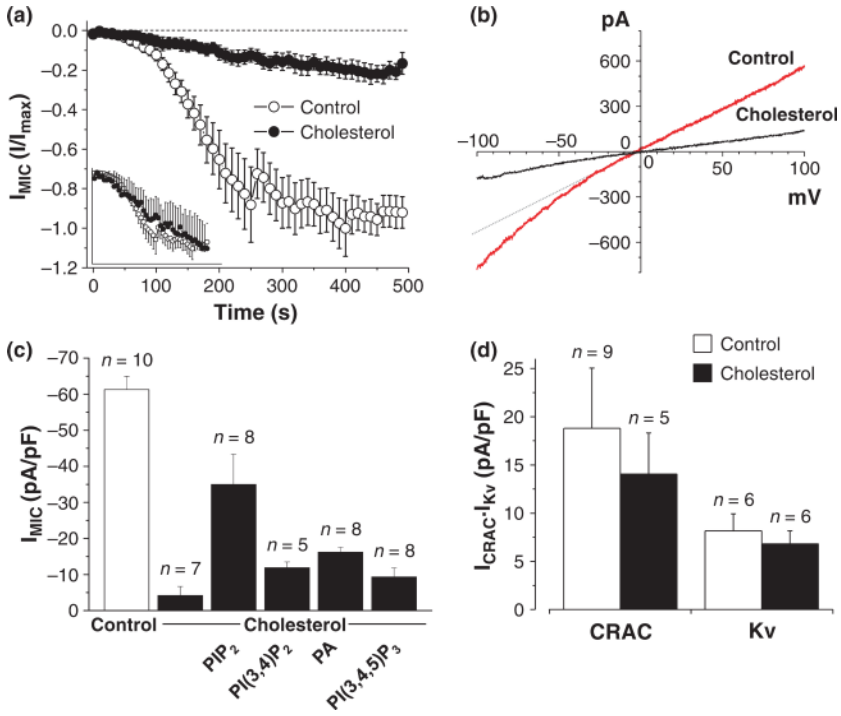

Fig. 1.

Inhibition of endogenous Mg^{2+}-inhibitory cation channel (MIC) currents by cholesterol enrichment. (a) Time-dependent activation profile of MIC currents. Currents at –100 mV were plotted in control ($n = 6$; ○) and cholesterol-treated HEK293 cells ($n = 6$; ●). Cells were pre-incubated for 1–2 h with 150 μM cholesterol before recordings. MIC currents were elicited by ramp pulses from –100 to +100 mV every 10 s using whole-cell configurations bathed in Ca^{2+}-free bath solution. The inset shows the normalized MIC currents from control and cholesterol-treated cells. Currents were normalized relative to the maximum current levels in each condition. (b) Current–voltage relationships of the MIC current. Currents were obtained in response to ramp pulses from –100 to +100 mV during a 200-ms period in control and cholesterol-treated cells. Currents were elicited 500 s after the formation of whole cell-configuration to induce full activation of MIC currents. A dotted line is drawn over the control current trace to show the inward rectification of the MIC current. (c) Recovery of MIC currents by phosphatidylinositol 4,5-bisphosphate (PIP_2) in cholesterol-treated HEK293 cells. In some recordings, 25 μM PIP_2, phosphatidylinositol 3,4-bisphosphate [$PI(3,4)P_2$], phosphatidic acid (PA), or phosphatidylinositol 3,4,5-trisphosphate [$PI(3,4,5)P_3$] was included in the pipette solution. (d) Effects of cholesterol enrichment on other endogenous currents from HEK293 cells. Ca^{2+} release-activated Ca^{2+} (CRAC) currents and voltage-dependent K^+ (Kv) currents were measured in control and cholesterol-treated HEK293 cells, and current density values (pA/pF) are presented.

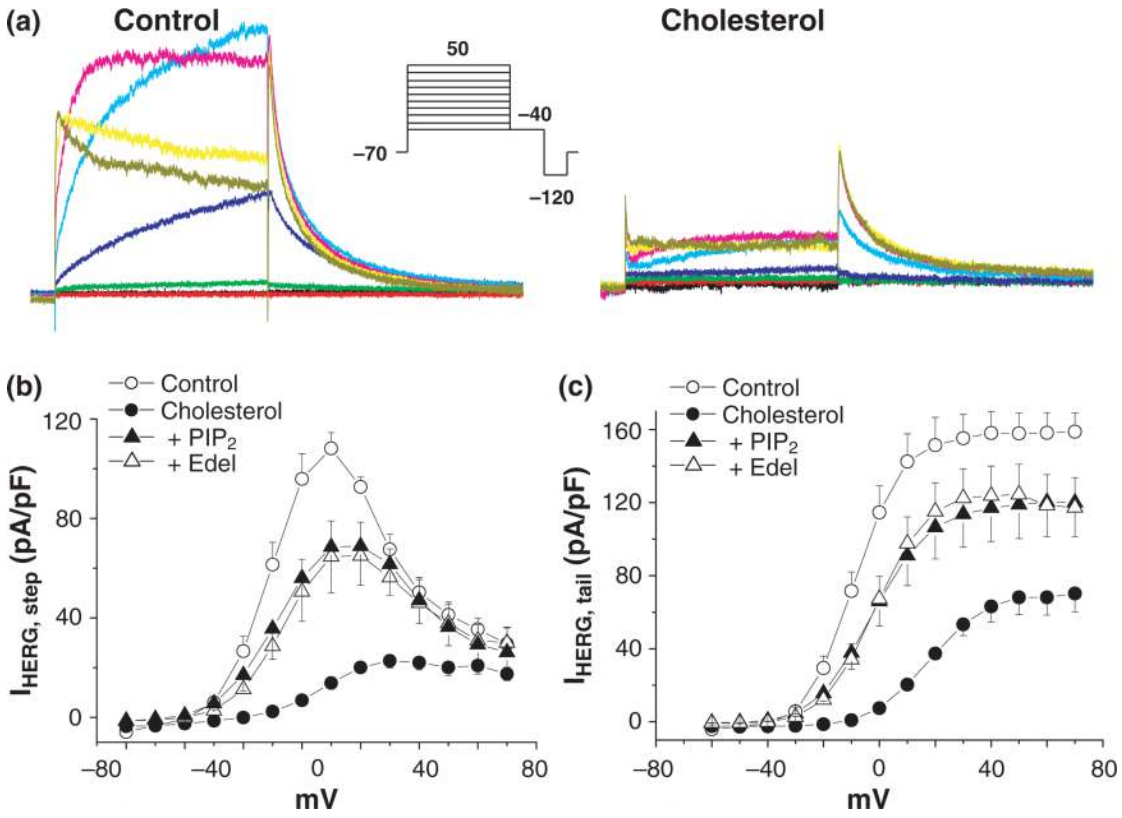

Fig. 2.

Inhibition of exogenously expressed ether-a-go-go-related gene (HERG) currents by cholesterol enrichment. (a) Representative HERG K^+ current traces are shown in control and cholesterol-treated HEK293 cells. Cells were pre-incubated for 1–2 h with 150 μM cholesterol before recordings. Depolarizing steps were applied from a holding potential of –70 mV to between –60 and +50 mV for 4 s, followed by a step to –40 mV to elicit currents. As more depolarized membrane potentials were applied, HERG K^+ currents were activated more rapidly, as evident in control current traces. (b, c) Averaged current–voltage relations obtained for HERG K^+ currents (n = 7). Currents were measured at the end of the depolarizing step ($I_{HERG,step}$) and for peak tail current amplitude ($I_{HERG,tail}$) following the step to –40 mV. This pulse protocol was applied at 15 s intervals. In some recordings in cholesterol-treated cells, 25 μM phosphatidylinositol 4,5-bisphosphate (PIP_2) was included in the pipette solution (+PIP_2). In some recordings, cells were treated with cholesterol along with phospholipase C inhibitor, 5 μM edelfosine (+Edel).

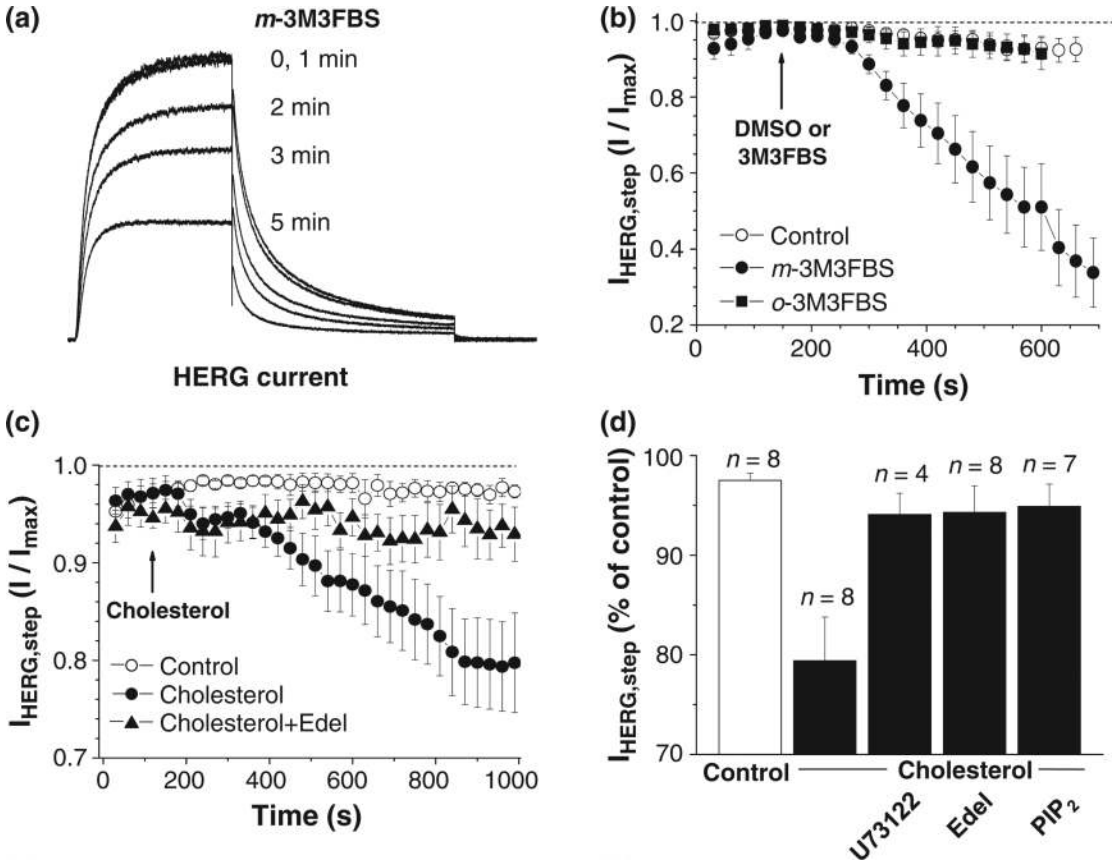

Fig. 3.

Inhibition of ether-a-go-go-related gene (HERG) currents by acute application of phospholipase C (PLC) activator and cholesterol. (a) The effect of acute application of a PLC activator on the HERG current. Representative current traces show HERG K^+ current before (0 min) and after (1, 2, 3 and 5 min) the application of the PLC activator, *m*-3M3FBS (25 μM). Currents were elicited by depolarizing voltage step to +30 mV from a holding potential of –70 mV for 4 s, followed by a step to –40 mV. (b) Steady state currents ($I_{HERG,step}$) were measured in different conditions. PLC activator (*m*-3M3FBS; $n = 6$) or non-active form (*o*-3M3FBS; $n = 8$) was added at the time indicated by the arrow. Vehicle (DMSO) was added for control ($n = 6$). (c) Steady state currents ($I_{HERG,step}$) were measured in different conditions. The effect of 150 μM cholesterol is shown (cholesterol; $n = 8$). In some cells, the PLC inhibitor edelfosine (10 μM) (cholesterol + Edel; $n = 8$), were included in whole-cell pipette solutions. Vehicle DMSO was added for control (control; $n = 8$). Cholesterol was added at the time indicated by the arrow. (d) Comparison of average steady state HERG K^+ currents expressed as % of control. The data were the same as in (c) except for the PLC inhibitors U73122 ($n = 4$). The presence of 25 μM PIP_2 in the pipette solution also blocked the inhibitory effect of cholesterol ($n = 7$).

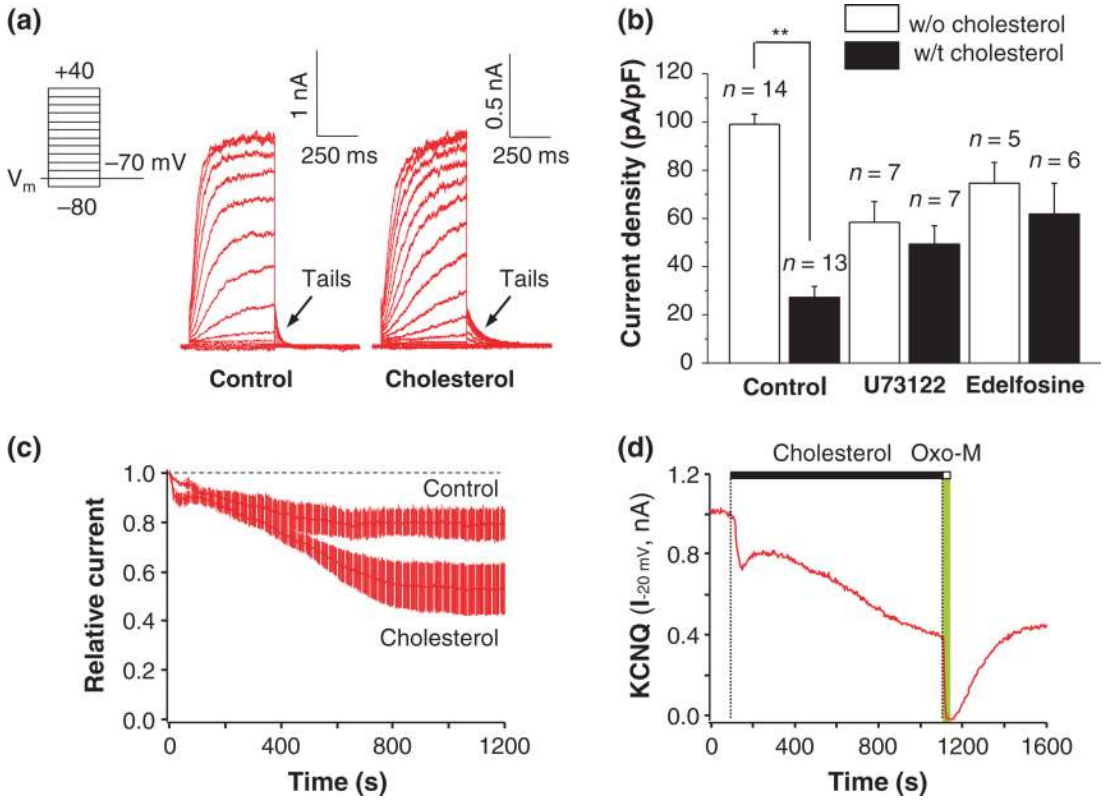

Fig. 4.

Inhibition of KCNQ current by cholesterol enrichment. (a) Inhibition of exogenously expressed KCNQ2/KCNQ3 K^+ current by cholesterol. Families of K^+ current elicited by voltage steps from –80 to +40 mV, in 10-mV intervals (see the pulse protocol), with or without incubation of 150 μM cholesterol for 1–2 h (Control vs. Cholesterol in the figure). The holding potential was –70 mV. (b) Current density measured immediately after whole-cell breakthrough in control and cholesterol-treated cells. Cells expressing KCNQ channels were preincubated at 37°C for 2 h in the presence or absence of cholesterol (150 μM). Control, 95.7 ± 14.6 pA/pF; cholesterol, 23.0 ± 6.4 pA/pF, $n = 7$. *$p < 0.01$. In some cells, U73122 (2.5 μM) or edelfosine (2.5 μM) was pre-incubated with or without cholesterol for 2 h at 37°C. (c) Time course of KCNQ current modulation by acute application of cholesterol (150 μM). Measurements started 3 min after breaking through to whole-cell recording at 23–25°C. Vertical bars are SEM. Control, $n = 3$; cholesterol, $n = 5$. (d) Modulation of KCNQ current by cholesterol and oxotremorine-M (Oxo-M). Whole-cell currents were recorded during the application of cholesterol (150 μM) and Oxo-M (10 μM).

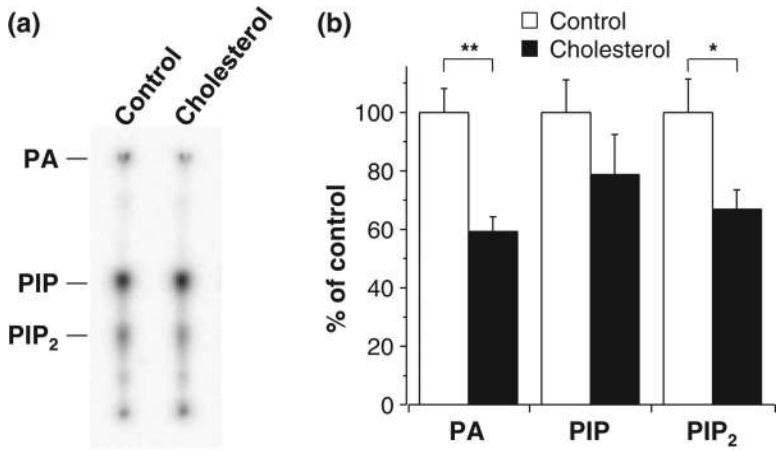

Fig. 5.

Down-regulation of phosphatidylinositol 4,5-bisphosphate (PIP_2) by cholesterol. (a) Alteration of PIP_2 metabolism in cholesterol-treated cells. TLC analysis of lipid extracts prepared either from control or cholesterol-treated (150 μM for 2 h) HEK293 cells. PIP, phosphatidylinositol 4-monophosphate. (b) Quantification of TLC data.